

Quantum anomalous Hall insulator of composite fermions in twisted bilayer graphene

Guangyue Ji¹ and Junren Shi^{1,2,*}

¹*International Center for Quantum Materials, Peking University, Beijing 100871, China*

²*Collaborative Innovation Center of Quantum Matter, Beijing 100871, China*

We theoretically study the realization of quantum anomalous Hall insulator (QAHI) of composite fermions (CFs) in the twisted bilayer graphene (TBG) system. We show that the moiré pattern in TBG is not only able to provide a commensurate moiré superlattice, but also a tunable effective periodic potential necessary for the realization, without the need of imposing an additional superstructure as in the conventional GaAs system. These make the TBG an ideal platform for realizing the QAHI of CFs. We establish the phase diagram with respect to tunable experimental parameters based on the Dirac CF theory. We find that the topological property of the system depends critically on the orbital magnetic susceptibility of CFs, which is not specified in the pristine Dirac CF theory. The experimental realization of QAHI of CFs would be helpful for unveiling the magnetic property of CFs and clarifying the issue.

Introduction The moiré pattern in van der Waals (vdW) heterostructures has attracted widespread investigations in both theoretical and experimental condensed matter physics. It provides us a powerful way of precisely controlling the electronic properties [1–4] and realizing exotic quantum states including the unconventional superconductor [5], Mott insulator [6, 7], and fractional Chern insulator [8]. Moreover, in the presence of a magnetic field, there is an interplay between the moiré potential and the magnetic length, and people have used this to study the quantum Hall physics subjected to a periodic modulation. In contrast to previous works mostly focused on the study of energy spectrums of non-interacting electrons, i.e., the Hofstadter’s butterfly [9–12], this work focuses on the quantum anomalous Hall insulator (QAHI) of composite fermions (CFs), which is a strongly-correlated topological state consisting of emergent quasiparticles in a Landau level [13].

A CF consists of an electron and $2p$ quantum vortices, and subjects to a reduced effective magnetic field [14]. In particular, at even-denominator magnetic filling $\nu_m = 1/2p$, the effective magnetic field vanishes, and the system is proposed to form a Fermi liquid of CFs (CFL) [15]. The CFL state has already been observed in various 2D electron systems including the graphene and its vdW heterostructure [16, 17]. Moreover, inspired by the Haldane model [18], it is proposed that imposing a proper electrostatic potential modulation on the CFL state, which is equivalent to an effective magnetic field modulation for CFs [15, 19], is able to induce the QAHI of CFs [13]. The exotic state is proposed to be able to exhibit fractional quantum Hall effect (FQHE) when $p > 1$. As a topological phase consisting of emergent quasiparticles in a strongly-correlated system, which is also proposed to lie in a duality web in $2 + 1$ dimension [20, 21], its novel properties are urged to be tested in experiment.

However, although the proposal of QAHI of CFs has attracted much attention, it has yet to be realized in exper-

iment as far as we know, let alone test its novel physical properties. The reason is that realizing the QAHI of CFs requires the length scale of the modulation potential to be commensurate with the magnetic length, which is difficult to realize in the conventional GaAs system. Besides, imposing a superstructure on the GaAs sample to construct the required modulation potential will inevitably affect the quality of the sample. These difficulties hinder the experimental realization of the QAHI of CF in the conventional GaAs system.

In this work, we will focus on its experimental realization in a moiré heterostructure, i.e., the twisted bilayer graphene (TBG) system instead. We show that the moiré pattern in TBG is not only able to provide a commensurate moiré superlattice, but also a tunable effective periodic potential necessary for the realization, without the need of imposing an additional superstructure as in the conventional GaAs system. These make the TBG an ideal platform for realizing the QAHI of CFs. Furthermore, we establish the phase diagram with respect to tunable experimental parameters based on the Dirac CF theory. We find that the topological property of the system depends critically on the orbital magnetic susceptibility of CFs, which is not specified in the pristine Dirac CF theory [22]. The experimental realization of QAHI of CFs will be helpful for unveiling the magnetic property of CFs and classifying the issue.

TBG system The QAHI of CFs was first proposed in Ref. [13]. According to the CF theory, we know CFs feel a reduced effective magnetic field: $B^* = B - 2pn_e\Phi_0$, where B is the external magnetic field, n_e is the electron density, $\Phi_0 = h/e$ is a quantum flux. At even-denominator magnetic filling $\nu_m \equiv n_e h/eB = 1/2p$, CFs feel zero effective magnetic field and form the CFL state. Furthermore, if one imposes a periodic scalar potential modulation on the system, it will induce an electron density modulation δn_e , which will further induce an effective magnetic field modulation δB^* . By tuning δB^* in analogy to the Haldane model, it is expected to realize the QAHI of CFs when integer CF Bloch bands are fully filled. The band filling factor is defined as $\nu_e \equiv n_e S$, where $S = 3\sqrt{3}L^2/2$ is the area of the hexagonal unit cell and L is the lat-

* junrenshi@pku.edu.cn

tice constant. Ref. [13] shows that there are two key conditions in realizing the QAHI of CFs. One is that the lattice constant L should be commensurate with the magnetic length $l_B = \sqrt{\hbar/eB}$. Concretely, it requires $L = \sqrt{4\pi\nu_e/3\sqrt{3}\nu_m}l_B$. The other is a proper periodic modulation, which should be able to fully open the gap at the Fermi surface and drive the system into an insulator.

The required conditions can be fulfilled in TBG system with the set-up shown in Fig. 1(a), where the TBG sample is encapsulated with two dual-gates [23]. This set-up has been widely used to study the properties of bilayer graphene [16, 23–25]. By tuning the voltages applied to the top and bottom gates V_t and V_b , one can independently tune the total electron density n_e and electrical displacement field D . Concretely, the electron density is given by $n_e = c_t V_t + c_b V_b$, where $c_t = \varepsilon_t/d_t$ ($c_b = \varepsilon_b/d_b$) is the unit-area capacitance of the top (bottom) gate and it depends on the dielectric constant and thickness of the dielectric layer between TBG and the top (bottom) gate. The electrical displacement field is given by $D = (c_t V_t - c_b V_b)/2$, which can be tuned to be as large as several volts per nanometer in experiment [23]. The electrical displacement field will further induce an interlayer bias Γ . For the AB-stacked bilayer graphene at the charge neutral point, a large band gap $\Delta \approx \Gamma \approx 0.25$ eV induced by the interlayer bias has already been observed in experiment [23]. This indicates the interlayer bias Γ is widely tunable. In the following, we will show that the two key conditions for realizing the QAHI of CFs can be fulfilled with the continuously tunable electron density n_e and interlayer bias Γ .

First, let's look at the commensurate condition. For a typical magnetic field $B \sim 10$ T, $L \sim 18$ nm for $\nu_m = 1/2$ and $\nu_e = 1$. The ratio between L and the carbon-carbon distance of graphene $a_0 \approx 1.42$ Å is $L/a_0 \sim 126$, which corresponds to a large superlattice. On the other hand, we know that the lattice constant of a TBG superlattice is determined by its twist angle θ : $L = a_0 |m - n|/2 \sin(\theta/2)$ [26], where the superlattice vector is set to be $\mathbf{L}_1 = m\mathbf{a}_1 + n\mathbf{a}_2$ and \mathbf{a}_i are the lattice vectors of the graphene. We have two ways to construct a large superlattice: one is large m and n and small $|m - n|$ with $\theta \sim 0$, and the other is large $|m - n|$ with $\theta \sim 30^\circ$ [2]. By tuning the twist angle θ , one can easily realize a large superlattice as shown in Fig. 1(b). Furthermore, by tuning the electron density n_e , one can realize the desired electron filling ν_e . Meanwhile, one can tune the applied magnetic field and realize the desired magnetic filling ν_m . In this way, one can precisely realize the required commensurate condition in this system.

Next, let's look at the periodic modulation condition. In the following, we will show that apart from providing us a moiré superlattice, the moiré pattern is also able to induce an effective period potential with tunable strength. The TBG consists of two layers of graphene with a relative rotation angle. The monolayer

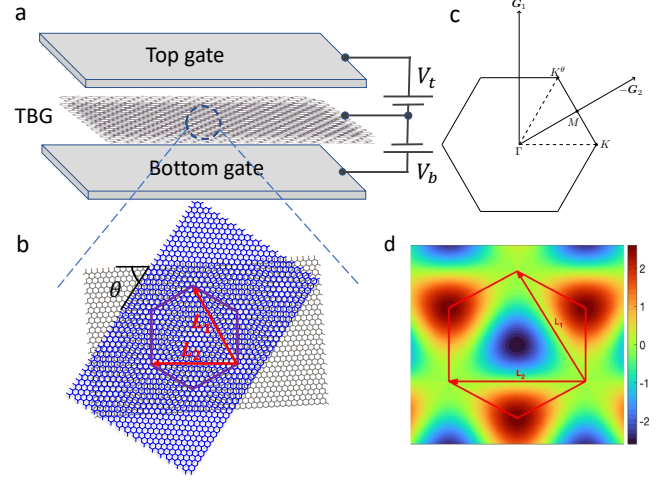


Figure 1. (a) Schematic of the device with the TBG encapsulated between two dual-gates. By tuning V_t and V_b , one can independently tune the electron density $n_e = c_t V_t + c_b V_b$ and the electrical displacement field $D = (c_t V_t - c_b V_b)/2$, where c_t (c_b) is the unit-area capacitance of the top (bottom) gate. (b) Moiré Superlattice of TBG. $\mathbf{L}_1 = (\sqrt{3}L/2)(-1, \sqrt{3})$ and $\mathbf{L}_2 = -\sqrt{3}L(1, 0)$ are its primitive lattice vectors. The lattice constant L can be tuned with the rotation angle θ . (c) First Brillouin zone. \mathbf{G}_1 and \mathbf{G}_2 are the reciprocal lattice vectors of the moiré superlattice. \mathbf{K} (\mathbf{K}') is the (rotated) Dirac point. (d) Spatial profiles of the periodic potential $V(\mathbf{r})$ in Eq. (4) with $|V_0| = 1$ and $\nu_m/\nu_e = 1/2$.

graphene is a honeycomb lattice of carbon atoms, of which each unit cell contains two inequivalent atoms denoted as A and B. In the reciprocal lattice space near the Dirac point $\mathbf{K} = (4\pi/3\sqrt{3}a_0)(1, 0)$, it can be described by the Dirac equation $H_G = -iv_e \boldsymbol{\sigma} \cdot \nabla$, where $\boldsymbol{\sigma} = (\sigma_x, \sigma_y)$ are Pauli matrices and $v_e \approx 1 \times 10^6$ m/s is the Fermi velocity [27]. For the other layer with rotation θ , its Hamiltonian is $H_G^\theta = \boldsymbol{\sigma}^\theta \cdot (-iv_e \nabla - \Delta \mathbf{K})$, where $\boldsymbol{\sigma}^\theta = e^{i\theta\sigma_z/2}(\sigma_x, \sigma_y)e^{-i\theta\sigma_z/2}$ are the rotated Pauli matrices, $\Delta \mathbf{K} = \mathbf{K}^\theta - \mathbf{K}$ is the displacement of the Dirac point (see Fig. 1c), and $\mathbf{K}^\theta = R(\theta)\mathbf{K}$ with $R(\theta)$ being the rotation matrix. Furthermore considering the interlayer hopping, we obtain the following Hamiltonian describing the TBG [1, 3, 9]:

$$H_{\text{TBG}} = \begin{pmatrix} -i\boldsymbol{\sigma} \cdot \nabla & T(\mathbf{r}) \\ [T(\mathbf{r})]^\dagger & \boldsymbol{\sigma}^\theta \cdot (-i\nabla - \Delta \mathbf{K}) \end{pmatrix}, \quad (1)$$

where $T(\mathbf{r}) = \omega \sum_{\mathbf{G}} T_{\mathbf{G}} e^{i\mathbf{G} \cdot \mathbf{r}}$ is the interlayer hopping matrix with

$$T_0 = \begin{pmatrix} 1 & 1 \\ 1 & 1 \end{pmatrix}, T_{-\mathbf{G}_1} = \begin{pmatrix} e^{i\phi_0} & 1 \\ e^{-i\phi_0} & e^{i\phi_0} \end{pmatrix}, \\ T_{-\mathbf{G}_1 - \mathbf{G}_2} = \begin{pmatrix} e^{-i\phi_0} & 1 \\ e^{i\phi_0} & e^{-i\phi_0} \end{pmatrix} \quad (2)$$

for the initial AB stacked structure, $\mathbf{G}_1 = \sqrt{3}R(-\pi/6)\Delta \mathbf{K}$ and $\mathbf{G}_2 = \sqrt{3}R(\pi/2)\Delta \mathbf{K}$ are the

reciprocal lattice vectors of the moiré superlattice, $\omega \approx 0.11$ eV is the hopping strength and $\phi_0 = 2\pi/3$ [1].

In the presence of a perpendicular magnetic field, the system will form Landau levels. For a monolayer graphene with a linear dispersion, its LL spectrum is $E_n = \text{sgn}(n)\sqrt{2|n|eB\hbar v_e}$ with $n = 0, \pm 1, \dots$. In this work, we focus on the spin and valley-polarized zeroth LL (ZLL), which is reasonable in experiment with strong magnetic field [16] and electric displacement field [28]. The wavefunctions in the ZLL of layer 1 have only A atom component, and we denote them as $|\psi_{1,m}\rangle = (|m\rangle, 0)^T$, where $|m\rangle$ are the LLL eigenstates of the conventional massive electron system. The ZLL eigenstates of layer 2 are related to layer 1 and given by $|\psi_{2,m}\rangle = e^{i\theta\sigma_z/2} e^{i\Delta\mathbf{K}\cdot\mathbf{r}} |\psi_{1,m}\rangle$. In the presence of the interlayer coupling $T(\mathbf{r})$, the ZLLs of the two layers will couple with each other. In the following, we will show that the interlayer coupling will induce an effective periodic potential.

In the presence of non-zero interlayer bias Γ , the layer ZLL energy degeneracy will be lifted. When Γ is much larger than the interlayer hopping strength ω , the two layers can be well seen as two isolated layers with the interlayer coupling acting as an effective perturbation potential. The effective potential induced by $T(\mathbf{r})$ can be derived by employing the perturbation theory. Its matrix element (accurate to the second order of ω) between any two states $\psi_{1,m}$ and $\psi_{1,m'}$ in the ZLL of layer 1 is

$$V_{mm'} = \frac{\omega^2}{\Gamma} \sum_{l, \mathbf{G}, \mathbf{G}'} T_{\mathbf{G}}^{11} (T_{\mathbf{G}'}^{11})^* \langle m | e^{i\mathbf{q}\cdot\mathbf{r}} | l \rangle \langle l | e^{-i\mathbf{q}'\cdot\mathbf{r}} | m' \rangle, \quad (3)$$

where $\mathbf{q} = \mathbf{G} + \Delta\mathbf{K}$. Note that $\sum_l |l\rangle\langle l|$ is in fact the conventional LLL projection operator \hat{P}_{LLL} [29]. By using the commutation relation of projected plane wave factors [29], one can show $\sum_l \langle m | e^{i\mathbf{q}\cdot\mathbf{r}} | l \rangle \langle l | e^{-i\mathbf{q}'\cdot\mathbf{r}} | m' \rangle = e^{-\frac{1}{2}i\mathbf{q}'\cdot\mathbf{r}} \langle m | e^{i(\mathbf{q}-\mathbf{q}')\cdot\mathbf{r}} | m' \rangle$, where $q = q_x + iq_y$ and $\bar{q} = q_x - iq_y$. By substituting it and the hopping matrix Eq. (2) into Eq. (3), we derive $V_{mm'} = \langle m | V(\mathbf{r}) | m' \rangle$ with the effective potential

$$V(\mathbf{r}) = V_0 \left(\sum_{i=1}^2 e^{i\mathbf{G}_i\cdot\mathbf{r}} + e^{-i(\mathbf{G}_1+\mathbf{G}_2)\cdot\mathbf{r}} \right) + \text{h.c.}, \quad (4)$$

where $V_0 = \frac{\omega^2}{\Gamma} \exp[-(|q|^2 l_B^2/2) e^{i2\pi/3}]$, $|q| = |\Delta\mathbf{K}| = 2|\mathbf{K}|\sin(\theta/2)$, and an irrelevant phase factor $e^{-i\phi_0}$ has been removed through a translation of the original point [30]. Furthermore, by using the commensurate condition, it can be simplified to be

$$V_0 = \frac{\omega^2}{\Gamma} \exp\left[\frac{\alpha}{\sqrt{3}}\right] \exp[-i\alpha], \quad (5)$$

where $\alpha = \frac{\pi}{3} \frac{\nu_m}{\nu_e}$ is the phase factor and it is determined by the ratio of magnetic and band filling factors. The spatial profile of $V(\mathbf{r})$ with $|V_0| = 1$ and $\nu_m/\nu_e = 1/2$ is

plotted in Fig. 1(d), and it is triangular. Since the interlayer bias Γ is widely tunable, the effective potential V_0 induced by the moiré pattern is also widely tunable. Thus, it is expected to fulfill the required periodic modulation condition without much difficulty.

Dirac composite fermions In the following, we study the QAHI of CFs subjected to the periodic potential Eq. (4) by adopting the Dirac CF theory, in which the particle-hole symmetry is explicit [22]. The Dirac CF theory treats CFs as neutral massless Dirac particles. The motion of Dirac CFs is governed by the Dirac equation $i\partial_t\psi = \hat{H}\psi$, where ψ is the Dirac CF spinor, and the Hamiltonian

$$\hat{H} = \boldsymbol{\sigma} \cdot (-i\boldsymbol{\partial} - \mathbf{a}(\mathbf{r})) + a_0(\mathbf{r})\sigma_0, \quad (6)$$

where $a^\mu = (a^0, \mathbf{a})$ are the internal gauge fields, σ_0 is the identity matrix, we have set $e = \hbar = v_{\text{CF}} = 1$ and will restore these constants when appropriate. Meanwhile, the CF system subjects to the constraints [22]

$$\rho_{\text{CF}} \equiv \langle \psi^\dagger \psi \rangle = \frac{B}{4\pi}, \quad (7)$$

$$\mathbf{j}_{\text{CF}} \equiv \langle \psi^\dagger \boldsymbol{\sigma} \psi \rangle = -\frac{1}{4\pi} \hat{z} \times \mathbf{E}, \quad (8)$$

where ρ_{CF} and \mathbf{j}_{CF} are the CF density and current, respectively, $\mathbf{B} = B\hat{z}$ and \mathbf{E} are the external electromagnetic fields, and $\langle \dots \rangle$ denotes the grand canonical ensemble average. The CF density is set by the external magnetic field, but not the electron density as assumed in the HLR theory [15]. It is a manifestation of the particle-vortex duality with the electron system. In the presence of the scalar potential $V(\mathbf{r})$, the CF current is fixed to be $\mathbf{j}_{\text{CF}} = (1/4\pi)\hat{z} \times \nabla V(\mathbf{r})$ according to Eq. (8). To induce a CF current satisfying this constraint, the internal magnetic field $\mathbf{b}(\mathbf{r})$ coupled to CFs needs to adjust accordingly. By tuning it properly, it is expected to realize the QAHI of Dirac CFs.

Different from systems governed by the Schrödinger equation, there exists a Dirac sea consisting of all negative-energy states. When a modulation is imposed on the system, not only positive-energy states will respond to it, but also the Dirac sea. In Ref. [31], Principi et al. show that the current response of the Dirac sea to a vector potential is divergent. Thus, to evaluate the physical response current, we shall regularize the system first.

We regularize the system by employing the Pauli-Villars regularization scheme for $(2+1)$ -dimensional massless Dirac fermions proposed by Redlich in Refs. [32, 33]. The regularization scheme is as follows. For a massless Dirac system, one can introduce two auxiliary massive systems with the Hamiltonian $\hat{H}_m = \hat{H} \pm m\sigma^3$, where m is the mass and its magnitude is required to be much larger than the chemical potential, i.e., $m \gg \mu$. By canceling out the divergent term in our massless system with the auxiliary systems, we obtain a finite regularized current

$$\mathbf{j}^{\text{R}} \equiv \mathbf{j}_{m=0} - (\mathbf{j}_m + \mathbf{j}_{-m})/2 + \nabla \times (\chi_m^{\text{mag}} \mathbf{b}), \quad (9)$$

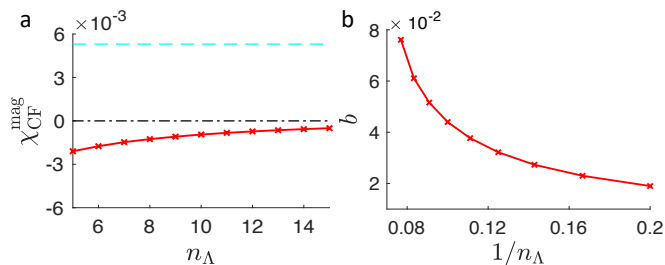


Figure 2. (a) CF magnetic susceptibility $\chi_{\text{CF}}^{\text{mag}}$ vs momentum cut-off $\Lambda = n_{\Lambda}|\mathbf{G}_i|$. The red line denotes the magnetic susceptibility of massless Dirac CFs. It approaches zero with the increase of the momentum cut-off. The horizontal cyan dashed line denotes $\chi_m^{\text{mag}} = 1/12\pi m$ with $m = 5$. (b) Induced Chern-Simons field strength (in unit of \hbar/eL^2) vs momentum cut-off. The modulation strength $|V_0|$ is set to be 5×10^{-3} . The induced Chern-Simons magnetic field is divergent with the increase of the momentum cut-off. It results from the zero CF magnetization susceptibility implicitly assumed in the Dirac CF theory.

where $\mathbf{j}_{\pm m}$ are the response currents of the massive systems. In addition to a divergent term, $\mathbf{j}_{\pm m}$ also contains finite Chern-Simons current and magnetization current $\nabla \times (\chi_m^{\text{mag}} \mathbf{b})$, where $\chi_m^{\text{mag}} = 1/12\pi m$ is the orbital magnetic susceptibility [34]. Since the Chern-Simons current is odd with respect to the mass, we eliminate it by introducing two auxiliary massive systems with opposite masses. Because the magnetization current is even with respect to the mass, we need to subtract its contribution manually as shown in Eq. (9).

To check the correctness of the above regularization scheme, we numerically calculate the orbital magnetization susceptibility $\chi_{\text{CF}}^{\text{mag}}$ of our massless Dirac system in the linear response region. First, we solve the eigenequation $\hat{H}\psi_{n,\mathbf{k}}(\mathbf{r}) = E_n(\mathbf{k})\psi_{n,\mathbf{k}}(\mathbf{r})$ subjected to a given \mathbf{b} for both massive and massless systems by employing the plane wave expansion method. Next, we calculate the current $\mathbf{j}_{m=0}$ and \mathbf{j}_m with derived eigenstates, and derive the regularized CF current \mathbf{j}^{R} by applying Eq. (9). Then, we can derive $\chi_{\text{CF}}^{\text{mag}}$ directly. The results show that $\chi_{\text{CF}}^{\text{mag}} \rightarrow 0$ with the increase of the momentum cut-off $\Lambda = n_{\Lambda}|\mathbf{G}_i|$ (see Fig. 2(a)). This is consistent with the analytic result that the orbital magnetic susceptibility of massless Dirac fermions at $\mu > 0$ is zero [34].

However, a zero CF magnetization susceptibility will lead to an infinite electron density response. The density susceptibility of electrons χ_e is inversely proportional to the magnetic susceptibility of CFs $\chi_{\text{CF}}^{\text{mag}}$ as follows [22]

$$\chi_e = \left(\frac{e}{2\hbar}\right)^2 \frac{1}{\chi_{\text{CF}}^{\text{mag}}}. \quad (10)$$

Note that though different CF effective theories treat CFs as different types of particles, the above relation is identical [22, 35, 36]. By substituting $\chi_{\text{CF}}^{\text{mag}} = 0$ into Eq. (10), one will obtain an infinite density response. That is to say a finite scalar modulation V will induce an infinite

electron density fluctuation, which is obviously unphysical. In our numerical study, we find that the induced magnetic field \mathbf{b} , which is proportional to the electron density fluctuation given by $b = B - 4\pi\rho_e$, is divergent with the increase of the cut-off as shown in Fig. 2(b). This also indicates that the density response of the system is divergent.

As we can see, the unphysical infinite density response results from the zero magnetization susceptibility of CFs implicitly assumed in the Dirac CF theory. In fact, the Dirac theory is a long-wavelength low-energy effective theory, while the magnetization is an effect of higher order [36, 37]. In the following, we proceed by introducing a finite orbital magnetic susceptibility of CFs $\chi_{\text{CF}}^{\text{mag}}$ into the Dirac CF theory and treating it as an extra parameter. In this case, there is an extra orbital magnetization current and the CF current in Eq. (8) needs to be modified to be

$$\mathbf{j}_{\text{CF}} = \langle \psi^\dagger \boldsymbol{\sigma} \psi \rangle + \nabla \times (\chi_{\text{CF}}^{\text{mag}} \mathbf{b}), \quad (11)$$

where the $\chi_{\text{CF}}^{\text{mag}} \mathbf{b}$ is the orbital magnetization. In this way, we solve the density response divergence problem in the pristine Dirac CF theory. Furthermore, by carefully tuning the periodic modulation potential $V(\mathbf{r})$, we show the system can form the QAH of Dirac CFs. Meanwhile, we find that the topological property of the system depends critically on the magnetic susceptibility of CFs.

QAH of Dirac CFs In the absence of modulation, CFs are free and form a Dirac cone with the Fermi wave vector $k_{\text{F}} = \sqrt{eB/\hbar}$. By folding the linear dispersion in the first BZ, we can obtain the energy bands of free Dirac CFs. They will touch at points of high symmetry. In the presence of a periodic modulation $V(\mathbf{r})$, energy degeneracies will be partially lifted. With an appropriate modulation strength and phase, the gap around the Fermi surface can be fully open, and the system forms an insulating state as shown in Fig. 3(b). The whole phase diagram for $\nu_{\text{m}} = 1/2$ is shown in Fig. 3(a). Note that the system will not form an insulating state at $\nu_e = 1$, because the degeneracy between the first two positive bands at K point can not be lifted with the triangular potential $V(\mathbf{r})$ shown in Fig. 1(d).

In the process of deriving the effective potential $V(\mathbf{r})$, it's assumed that the interlayer hopping strength ω is much smaller than the interlayer bias Γ and can be treated as a perturbation. Now, let's check its rationality. In the case of $\nu_{\text{m}} = 1/2$ and $\nu_e = 2$, the ratio between ω and the critical bias Γ_c is $\omega/\Gamma_c \approx 0.6\hbar v_{\text{CF}}/L\omega$, where we have set the magnetic susceptibility of CFs $\chi_{\text{CF}}^{\text{mag}} = -1/8\pi m_{\text{CF}}$ as done in Refs. [35, 36] and m_{CF} is the effective mass of CFs [15, 19]. By substituting the CF velocity $v_{\text{CF}} = \hbar k_{\text{F}}/m_{\text{CF}} \approx (7.2/\epsilon) \times 10^5$ m/s and the commensurate lattice constant $L = \sqrt{4\pi\nu_e/3\sqrt{3}\nu_{\text{m}}l_B}$ into the ratio, we obtain $\omega/\Gamma_c \approx (3.2/\epsilon) \times 10^{-2} B^{1/2}$, where ϵ is the dielectric constant and it is determined by the substrates. For the typical experimental parameters $\epsilon \sim 3 - 15$ and $B \sim 10$ T [38], $\omega/\Gamma_c \ll 1$. Thus, there is a wide range

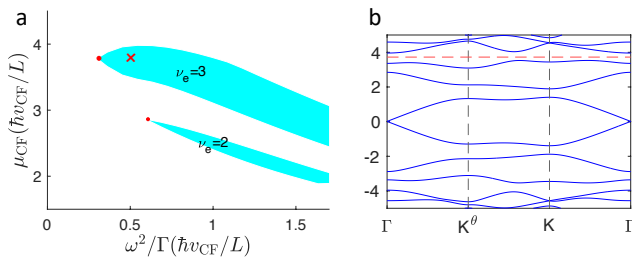


Figure 3. (a) Phase diagrams of Dirac CFs for $\nu_m = 1/2$. The area of insulating states is marked with cyan. μ_{CF} is the chemical potential of CFs. The energy unit is $\hbar v_{\text{CF}}/L$. The magnetic susceptibility of CFs is set to be $\chi_{\text{CF}}^{\text{mag}} = -1/8\pi m_{\text{CF}}$. The critical bias (marked with red circles) is $\Gamma_c \approx \omega^2/(0.6\hbar v_{\text{CF}}/L) \approx 3.4\epsilon B^{-1/2}$ eV for $\nu_e = 2$ and $\Gamma_c \approx 8.4\epsilon B^{-1/2}$ eV for $\nu_e = 3$. (b) Energy bands of Dirac CFs at $\omega^2/\Gamma = 0.5$ and $\nu_e = 3$ (marked with a cross in (a)). It can be seen that the energy degeneracy near the Fermi surface has been fully lifted with the given periodic potential modulation. The CF Hall conductivity of the insulating state is $-e^2/2h$ ($+e^2/2h$) for $\Gamma\chi_{\text{CF}}^{\text{mag}} < 0$ ($\Gamma\chi_{\text{CF}}^{\text{mag}} > 0$). The corresponding electron Hall conductivity is e^2/h (0).

of Γ satisfying $\omega \ll \Gamma < \Gamma_c$. Since the interlayer bias Γ is widely tunable, e.g., $\Gamma \approx 0.25$ eV $> \omega \approx 0.11$ eV has already been realized in experiment [23], it is reasonable to treat the interlayer hopping as a perturbation to the CFL state.

Next, we analyze the topological property of the insulating state by calculating its Hall conductivity. For a non-degenerate band, one can evaluate its Hall conductivity by applying the TKNN formula: $\sigma^{xy} = -\mathcal{C}/2\pi = -(1/2\pi) \int_{\text{BZ}} (d^2k/2\pi) \Omega_{k_x k_y}$, where $\Omega_{k_x k_y}$ is the Berry curvature in the momentum space, and \mathcal{C} is the Chern number of the band [39]. Naively, one expects to derive the Hall conductivity of the system by summing up the Chern number of all occupied positive bands. However, this is incorrect for the Dirac system because it ignores the contribution of the filled Dirac sea. To correctly evaluate the Hall conductivity of the Dirac system, we regularize the system by introducing auxiliary massive systems as done in Eq. (9). The expression of the regularized Hall conductance is given by

$$\sigma_{\text{CF}}^{xy} \equiv \sigma_{m=0}^{xy} - (\sigma_m^{xy} + \sigma_{-m}^{xy})/2, \quad (12)$$

where $\sigma_{m=0}^{xy}$ (σ_m^{xy}) is the total Hall conductivity of all occupied bands below the chemical potential μ_{CF} ($\ll m$) of the massless (massive) Dirac system. In numerical calculations, we evaluate σ_m^{xy} by setting a momentum cut-off $\Lambda = n_\Lambda |\mathbf{G}_i|$ as done before. Since σ_{CF}^{xy} is a topological quantity independent of the cut-off, it can be easily evaluated by setting a small n_Λ . Finally, we obtain the Hall conductivity of the insulating state, and it is (in unit of e^2/h)

$$\sigma_{\text{CF}}^{xy} = \begin{cases} -\frac{1}{2}, & \text{for } \Gamma\chi_{\text{CF}}^{\text{mag}} < 0 \\ +\frac{1}{2}, & \text{for } \Gamma\chi_{\text{CF}}^{\text{mag}} > 0 \end{cases}. \quad (13)$$

The half-integer quantization is a character of Dirac particles [40, 41]. It can be seen that the Hall conductivity of the system critically depends on the orbital magnetization susceptibility of CFs. The reason is that the induced internal magnetic field are opposite for positive and negative $\chi_{\text{CF}}^{\text{mag}}$.

With the CF Hall conductivity determined, we can derive the electron Hall conductivity by applying the conductivity transformation relation $\sigma_e^{xy} = e^2/2h - (e^2/2h)^2/\sigma_{\text{CF}}^{xy}$ [22]. By substituting the CF conductivity Eq. (13) into the relation, we obtain the electron Hall conductivity (in unit of e^2/h)

$$\sigma_e^{xy} = \begin{cases} 1, & \text{for } \Gamma\chi_{\text{CF}}^{\text{mag}} < 0 \\ 0, & \text{for } \Gamma\chi_{\text{CF}}^{\text{mag}} > 0 \end{cases}. \quad (14)$$

For $\Gamma\chi_{\text{CF}}^{\text{mag}} < 0$, its Hall conductivity is nonzero and the insulating state is a topological insulator. Thus, the effective periodic potential induced by the interlayer hopping of the TBG system can indeed drive the CFL state into the QAHI of CFs.

In this work, we focus on the TBG system and the effective potential given by Eq. (4). In fact, the phase and strength of the effective potential can be further tuned by coupling more layers [4, 42, 43]. By using the interference between effective potentials induced by different layers, it is flexible to realize a desired potential. In this case, it is also possible to construct a hexagonal periodic potential and realize the QAHI of CFs at $\nu_e = 1$. Besides, one can also tune the effective potential by other methods, including coupling to substrates and tuning the strain [11, 24, 44, 45]. In short, the moiré pattern in vdW heterostructures provides us a powerful way of controlling the electronic properties to realize the QAHI of CFs.

For the theoretical part, a full understanding of orbital magnetic susceptibility of CFs is still absent and relevant investigations are rare. There even exists a misconception that its effect on observable physical quantities is negligible. However, we reveal that it in fact plays a central role in the QAHI of CFs. In particular, the zero magnetic susceptibility of CFs implicitly assumed in the Dirac theory will lead to an unphysical infinite density response. Thus, the experimental realization of the QAHI of CFs would be helpful for unveiling the magnetic property of CFs and clarifying the issue.

Summary In summary, we show that the moiré superlattice and effective periodic potential induced by the moiré pattern make TBG an ideal platform for realizing the QAHI of CFs. We establish the phase diagram with respect to tunable experimental parameters based on the Dirac CF theory. We find that the topological property of the system depends critically on the orbital magnetic susceptibility of CFs, which is not specified in the pristine Dirac CF theory. The experimental realization of QAHI of CFs would be helpful for clarifying the issue.

ACKNOWLEDGMENTS

G.J. and J.S. thank Qian Niu, Di Xiao, Jing-Yuan Chen, Yinhan Zhang, Haoran Chen and Xuesong Hu for

valuable discussions. This work is supported by the National Basic Research Program of China (973 Program) Grants No. 2018YFA0305603 and No. 2021YFA1401900 and the National Science Foundation of China Grant No. 12174005.

-
- [1] J. M. B. Lopes dos Santos, N. M. R. Peres, and A. H. Castro Neto, *Phys. Rev. Lett.* **99**, 256802 (2007).
- [2] G. Trambly de Laissardière, D. Mayou, and L. Magaud, *Nano Lett.* **10**, 804 (2010).
- [3] R. Bistritzer and A. H. MacDonald, *Proceedings of the National Academy of Sciences* **108**, 12233 (2011).
- [4] S. Carr, S. Fang, and E. Kaxiras, *Nature Reviews Materials* **5**, 748 (2020).
- [5] Y. Cao, V. Fatemi, S. Fang, K. Watanabe, T. Taniguchi, E. Kaxiras, and P. Jarillo-Herrero, *Nature* **556**, 43 (2018).
- [6] Y. Cao, V. Fatemi, A. Demir, S. Fang, S. L. Tomarken, J. Y. Luo, J. D. Sanchez-Yamagishi, K. Watanabe, T. Taniguchi, E. Kaxiras, R. C. Ashoori, and P. Jarillo-Herrero, *Nature* **556**, 80 (2018).
- [7] G. Chen, L. Jiang, S. Wu, B. Lyu, H. Li, B. L. Chittari, K. Watanabe, T. Taniguchi, Z. Shi, J. Jung, Y. Zhang, and F. Wang, *Nat. Phys.* **15**, 237 (2019).
- [8] Y. Xie, A. T. Pierce, J. M. Park, D. E. Parker, E. Khalaf, P. Ledwith, Y. Cao, S. H. Lee, S. Chen, P. R. Forrester, K. Watanabe, T. Taniguchi, A. Vishwanath, P. Jarillo-Herrero, and A. Yacoby, *Nature* **600**, 439 (2021).
- [9] R. Bistritzer and A. H. MacDonald, *Phys. Rev. B* **84**, 035440 (2011).
- [10] C. R. Dean, L. Wang, P. Maher, C. Forsythe, F. Ghahari, Y. Gao, J. Katoch, M. Ishigami, P. Moon, M. Koshino, T. Taniguchi, K. Watanabe, K. L. Shepard, J. Hone, and P. Kim, *Nature* **497**, 598 (2013).
- [11] B. Hunt, J. D. Sanchez-Yamagishi, A. F. Young, M. Yankowitz, B. J. LeRoy, K. Watanabe, T. Taniguchi, P. Moon, M. Koshino, P. Jarillo-Herrero, and R. C. Ashoori, *Science* **340**, 1427 (2013).
- [12] L. A. Ponomarenko, R. V. Gorbachev, G. L. Yu, D. C. Elias, R. Jalil, A. A. Patel, A. Mishchenko, A. S. Mayorov, C. R. Woods, J. R. Wallbank, M. Mucha-Kruczynski, B. A. Piot, M. Potemski, I. V. Grigorieva, K. S. Novoselov, F. Guinea, V. I. Fal'ko, and A. K. Geim, *Nature* **497**, 594 (2013).
- [13] Y. Zhang and J. Shi, *Phys. Rev. Lett.* **113**, 016801 (2014).
- [14] J. K. Jain, *Phys. Rev. Lett.* **63**, 199 (1989).
- [15] B. I. Halperin, P. A. Lee, and N. Read, *Phys. Rev. B* **47**, 7312 (1993).
- [16] J. I. A. Li, C. Tan, S. Chen, Y. Zeng, T. Taniguchi, K. Watanabe, J. Hone, and C. R. Dean, *Science* **358**, 648 (2017).
- [17] A. A. Zibrov, C. Kometter, H. Zhou, E. M. Spanton, T. Taniguchi, K. Watanabe, M. P. Zaletel, and A. F. Young, *Nature* **549**, 360 (2017).
- [18] F. D. M. Haldane, *Phys. Rev. Lett.* **61**, 2015 (1988).
- [19] J. Jain, *Composite Fermions* (Cambridge University Press, 2007).
- [20] N. Seiberg, T. Senthil, C. Wang, and E. Witten, *Annals of Physics* **374**, 395 (2016).
- [21] T. Senthil, D. T. Son, C. Wang, and C. Xu, *Physics Reports* **827**, 1 (2019).
- [22] D. T. Son, *Phys. Rev. X* **5**, 031027 (2015).
- [23] Y. Zhang, T.-T. Tang, C. Girit, Z. Hao, M. C. Martin, A. Zettl, M. F. Crommie, Y. R. Shen, and F. Wang, *Nature* **459**, 820 (2009).
- [24] E. M. Spanton, A. A. Zibrov, H. Zhou, T. Taniguchi, K. Watanabe, M. P. Zaletel, and A. F. Young, *Science* **360**, 62 (2018).
- [25] H. Polshyn, Y. Zhang, M. A. Kumar, T. Soejima, P. Ledwith, K. Watanabe, T. Taniguchi, A. Vishwanath, M. P. Zaletel, and A. F. Young, *Nature Physics* **18**, 42 (2022).
- [26] P. Moon and M. Koshino, *Phys. Rev. B* **85**, 195458 (2012).
- [27] A. H. Castro Neto, F. Guinea, N. M. R. Peres, K. S. Novoselov, and A. K. Geim, *Rev. Mod. Phys.* **81**, 109 (2009).
- [28] K. Huang, H. Fu, D. R. Hickey, N. Alem, X. Lin, K. Watanabe, T. Taniguchi, and J. Zhu, *Phys. Rev. X* **12**, 031019 (2022).
- [29] S. M. Girvin and T. Jach, *Phys. Rev. B* **29**, 5617 (1984).
- [30] Y. Zhang, Y. Gao, and D. Xiao, *Phys. Rev. B* **101**, 041410 (2020), arXiv:1910.09001 [cond-mat].
- [31] A. Principi, M. Polini, and G. Vignale, *Phys. Rev. B* **80**, 075418 (2009).
- [32] A. N. Redlich, *Phys. Rev. Lett.* **52**, 18 (1984).
- [33] A. N. Redlich, *Phys. Rev. D* **29**, 2366 (1984).
- [34] M. Koshino and T. Ando, *J. Phys.: Conf. Ser.* **334**, 012005 (2011).
- [35] C. Wang, N. R. Cooper, B. I. Halperin, and A. Stern, *Phys. Rev. X* **7**, 031029 (2017).
- [36] G. Ji and J. Shi, *Phys. Rev. Research* **3**, 043055 (2021).
- [37] G. Ji and J. Shi, *Phys. Rev. Research* **2**, 033329 (2020).
- [38] C. Töke and J. K. Jain, *Phys. Rev. B* **75**, 245440 (2007).
- [39] D. J. Thouless, M. Kohmoto, M. P. Nightingale, and M. den Nijs, *Phys. Rev. Lett.* **49**, 405 (1982).
- [40] A. M. J. Schakel, *Phys. Rev. D* **43**, 1428 (1991).
- [41] G. P. Mikitik and Y. V. Sharlai, *Phys. Rev. Lett.* **82**, 2147 (1999).
- [42] C. H. Lui, Z. Li, K. F. Mak, E. Cappelluti, and T. F. Heinz, *Nature Phys* **7**, 944 (2011).
- [43] W. Bao, L. Jing, J. Velasco, Y. Lee, G. Liu, D. Tran, B. Standley, M. Aykol, S. B. Cronin, D. Smirnov, M. Koshino, E. McCann, M. Bockrath, and C. N. Lau, *Nature Phys* **7**, 948 (2011).
- [44] S. Y. Zhou, G.-H. Gweon, A. V. Fedorov, P. N. First, W. A. de Heer, D.-H. Lee, F. Guinea, A. H. Castro Neto, and A. Lanzara, *Nature Mater* **6**, 770 (2007).
- [45] S.-M. Choi, S.-H. Jhi, and Y.-W. Son, *Nano Lett.* **10**, 3486 (2010).